Ceramics International 44 (2018) 6232–6241

Contents lists available at ScienceDirect

Ceramics International

journal homepage: www.elsevier.com/locate/ceramint

An investigation on the mechanism and reaction sequence of scheelite-magnesium mixtures during mechanical milling

Hossein yavari Mehrabani, Abolfazl Babakhani*

Department of Materials Science and Metallurgical Engineering, Engineering Faculty, Ferdowsi University of Mashhad, Postal code: 9177948974, Mashhad, Islamic Republic of Iran

ARTICLE INFO

Keywords:
Mechanically-induced self-propagating reaction
Scheelite
Planetary ball mill

ABSTRACT

The mechanism of mechanically-induced self-propagating reaction (MSR) of scheelite with magnesium during reactive ball milling was investigated using in-situ monitoring of the vial temperature, X-ray diffraction analysis and field emission scanning electron microscopy. Temperature variations of the vial versus milling time curves showed unusual behaviors in comparison to the reported patterns in literature. It is found that the main reason for these exceptional temperature behaviors is sublimation-deposition of magnesium. X-ray diffraction patterns of milled scheelite-magnesium mixtures revealed the formation of intermediate phases during MSR. The sequence of scheelite-magnesium reaction appeared as $CaWO_4 \rightarrow Ca_3WO_6 \rightarrow Ca_2MgWO_6 \rightarrow WO_3.x \rightarrow W$. Atomic force microscopy showed that the final product contains nanosize particles that are smaller than 50 nm.

1. Introduction

Tungsten has exceptional position amongst the elements due to its unique properties such as high melting point, lowest coefficient of expansion, highest tensile strength at temperatures over 1650 °C and high density [1,2]. More than 60% of tungsten consumption is in the form of tungsten carbide. Cemented carbide, also called hard metal is the most important usage for tungsten carbide. These materials are made by cementing hard WC grains in a binder matrix of tough cobalt (or Fe-Ni) by liquid phase sintering. As a result, hard metals combine high strength, hardness and large toughness [2,3].

The main primary resources of tungsten and its compounds such as tungsten carbide are scheelite ($CaWO_4$) and wolframite [Fe (Mn) WO_4] [4,5]. These ores are enriched by physical beneficiation to obtain concentrate assaying around 60% WO_3. Hydrometallurgy is the most preferred method for scheelite processing. In these methods, processing of scheelite starts by converting tungsten value of the ore to the soluble intermediate compounds such as ammonium paratungstate (APT). APT is then converted into WO_3 which is subsequently reacted with H_2 or carbon to produce tungsten and tungsten carbide respectively [6]. Hydrometallurgical extraction of tungsten includes several steps with various parameters which makes the process difficult. Additionally these methods produce waste waters that can threaten the environment. Thus various investigations have been carried out to suggest a process with lower environmental impacts. One of the suggested processes is mechanically-induced self-propagating reaction (MSR) that can be characterized by its short processing time. A variety of materials such as metals, ceramics and composites can be produced by MSR method. MSR is a kind of self-propagating high temperature synthesis in which the needed energy to ignite the reaction is provided by mechanical milling [7,8].

During the early stages of mechanical milling, mixing and particle refinement of powders occur. This is accompanied by the formation of fresh surfaces, high plastic strains and high densities of vacancies and dislocations. These crystal imperfections act as chemically active sites that can facilitate the ignition of MSR. When the internal energy and reactivity of the system reach a critical state, reaction is ignited by a collision between balls or a ball and the wall of vial. The ignition is accompanied by formation of a combustion front that propagates throughout the powder instantaneously [9,10].

In-situ temperature monitoring of the milling vial is an appropriate tool to realize events inside the vial. The output of this monitoring system is a temperature-milling time curve. These time-temperature curves provide various information that can be useful for researchers in process interpretation. Nevertheless, the in-situ temperature monitoring technique is generally limited to determining the mode of reactions (gradual or MSR), while it can be used as a beneficial technique to study MSR systems in more details. For instance, some systems have shown unusual temperature behaviors during reactive milling, while the researchers do not provide any explanation about the reasons [11,12].

Synthesis of W and WC through MSR have been investigated by researchers using WO_3 as precursor, but many of them have focused on the feasibility of reaction and characterization of products [13–15].

* Corresponding author.

https://doi.org/10.1016/j.ceramint.2018.01.008
Received 10 December 2017; Received in revised form 1 January 2018; Accepted 2 January 2018
Available online 03 January 2018

However, it is reported that the synthesis of WC via MSR includes two main steps. The first is synthesis of metallic tungsten by self-propagating reaction and the second step is formation of WC by reaction of tungsten and carbon during subsequent milling [13,16]. Accordingly, the aim of the present study is to investigate the first step.

Despite the cost advantages of using scheelite as precursor, few attempts have been carried out to investigate the mechanism of reactive ball milling of scheelite to produce W or WC [17]. Therefore, scheelite was used as the precursor in the present investigation. Additionally, magnesium powder was used as reducer metal in the milling process. Similar experiments were also carried out on the scheelite-aluminum system to compare the obtained results.

It is reported that the heat and products of MSR can affect the subsequent formation of WC. Therefore, carbon was eliminated in the present investigation to prevent overlapping of various reactions that can make describing the mechanism more difficult. Experiments in the presence of carbon have been carried out and will be discussed elsewhere.

2. Experimental procedure

Synthetic scheelite was obtained by using the analytical grade of hydrated sodium tungstate ($Na_2WO_4{\cdot}2H_2O$) and hydrated calcium chloride ($CaCl_2{\cdot}2H_2O$). Equimolar quantities of $Na_2WO_4{\cdot}2H_2O$ and $CaCl_2{\cdot}2H_2O$ were dissolved in 60 °C distilled water in separate beakers. $CaWO_4$ was precipitated according to reaction 1 by gradual addition of $CaCl_2$ solution into the beaker containing Na_2WO_4 solution at constant stirring speed. The Synthesized $CaWO_4$ was allowed to settle and then supernatant was decanted. The precipitant was washed with distilled water repeatedly to remove NaCl -that forms as by product- and probable unreacted Na_2WO_4 and $CaCl_2$. The synthesized scheelite was dried for 5 h in 140 °C and finally was grinded to break up any agglomerate.

$$Ca^{2+} + (WO4)^{2-} = CaWO_{4(s)} \quad (1)$$

Synthesized scheelite was characterized by X-ray diffractometry and Raman spectroscopy to ensure the similarity with natural crystal of scheelite.

This study is based on the in-situ temperature monitoring of the milling vial. This matter necessitates using a high resolution, high response speed and accurate temperature sensor and electrical circuit, whereas commercial temperature monitoring systems use types of thermocouples that have problems such as delay in signal transmission and low sensing resolution. Therefore the temperature of vial was monitored using a self-designed temperature data logger. DS18B20 digital temperature sensor with 0.1 °C resolution was used in this data logger. The thickness of the lid between sensor and inner surface of vial was just 1 mm. The data was transmitted to the stationary receiver which send them to the MATLAB R2012a software through a serial interface. Programing of microcontrollers in the data logger and data receiver were carried out using Atmel studio software. It should be noted that the obtained graphs were smoothed in MATLAB software.

The stoichiometric reactions of scheelite with magnesium and aluminum can be considered as follows:

$$CaWO_4 + 3\,Mg \rightarrow W + 3\,MgO + CaO \quad (2)$$

$$CaWO_4 + 2\,Al \rightarrow W + Al_2O_3 + CaO \quad (3)$$

Based on Eqs. (2) and (3), scheelite was mixed with various molar ratios of magnesium and aluminum according to Table 1. Powders were loaded in a 200 ml hardened steel vial. The mass of the samples were kept constant (4.12 g) in all samples. Three sizes of hardened steel balls (6, 8 and 10 mm) were used in the process with ball to powder ratio of 30:1. The vial: supporting disk rotation velocity ratio was 2:1 and the supporting disk speed was 250 rpm. Two groups of milling experiments were performed. In the first group of samples, the ball mill was turned off immediately after observing an abrupt temperature increase, while the second group of samples were milled for 60 min without any interruption.

Table 1
Powder mixture of 1 mol scheelite and various amounts of Mg or Al milled for various times.

Sample	Composition	Milling time	Sample	Composition	Milling time
0.8Mg	2.4 mol Mg	until MSR moment	**0.8Al**	1.6 mol Al	until MSR moment
0.8Mg60	2.4 mol Mg	60 min	**0.8Al60**	1.6 mol Al	60 min
1Mg	3 mol Mg	until MSR moment	**1Al**	2 mol Al	until MSR moment
1Mg60	3 mol Mg	60 min	**1Al60**	2 mol Al	60 min
1.2Mg	3.6 mol Mg	until MSR moment	**1.2Al**	2.4 mol Al	until MSR moment
1.2Mg60	3.6 mol Mg	60 min	**1.2Al60**	2.4 mol Al	60 min
1.4Mg	4.2 mol Mg	until MSR moment	**1.4Al**	2.8 mol Al	until MSR moment
1.4Mg60	4.2 mol Mg	60 min	**1.4Al60**	2.8 mol Al	60 min

Samples were analyzed by X-ray diffraction (EXPLORER GNR analytical instrument group) equipped with a plane monochromator using Cu Kα radiation (λ = 1.5418 A). Diffraction patterns were acquired using a count time of 1 s per 0.02° step. Powders were imaged using a field emission scanning electron microscope (FESEM) incorporating energy dispersive X-ray spectroscope (MIRA3 TESCAN). Raman spectroscopy was performed by using a 623 nm laser. The raman spectra were recorded in the range between 100 and 1000 cm^{-1}. Finally particle size was evaluated by an atomic force microscope (JPK NanoWizard II) using a mica substrate.

3. Result and discussion

3.1. Thermodynamic aspects

Table 2 shows the thermodynamic characteristics belonging to reaction 2 and 3. The value of standard Gibbs free energy determines whether a reaction can occur in the forward direction or not. Negative values of ΔG° indicate that the thermodynamic conditions are provided for proceeding of both reactions in the forward direction. It can be seen that both reactions are highly exothermic while reaction 2 release 130 kJ/mol more heat than reaction 3. Therefore the adiabatic temperature of reaction 2 is higher than that of reaction 3. According to the Merzhanov criterion, if the $T_{ad} > 1800$ K, the reactions can occur in a self-propagating high temperature synthesis (SHS) mode [18]. Herein, the calculated adiabatic temperatures of both reactions are higher than 1800 K and theoretically they can occur in SHS mode [19,20].

Fig. 1 shows the calculated adiabatic temperature of mixtures containing scheelite and various amounts of Mg or Al. It can be seen that the adiabatic temperature of scheelite-magnesium mixtures is higher than scheelite-aluminum ones in similar ratios. With regard to this figure, the maximum adiabatic temperatures are attained in stoichiometric mixtures which are 3533 K and 3142 K for Mg and Al systems, respectively. Since the adiabatic temperature of all mixtures is higher than 1800 K, SHS in these systems is likely to occur.

The high adiabatic temperature of the reactions may cause phase transformations in the reactants. Thus physical characteristics of the reactants should be considered in mechanism investigations.

Table 2
Thermodynamic information of Scheelite-magnesium and Scheelite-aluminum reactions.

Reaction number	ΔG°(kJ/mol)	ΔH° (kJ/mol)	T_{ad} (K)
2	−775	−820	3533
3	−653	−691	3142

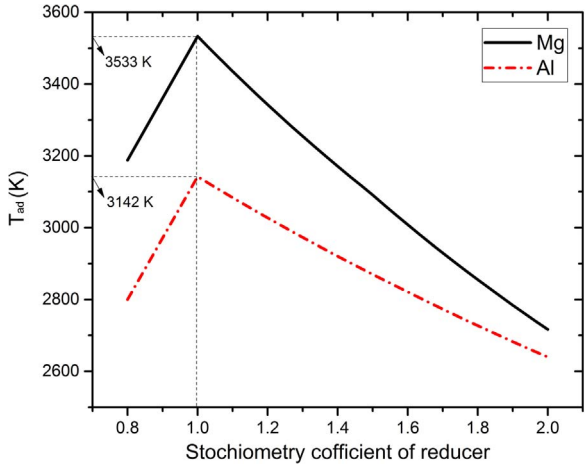

Fig. 1. Adiabatic temperature of mixtures containing scheelite and various amounts of Mg or Al.

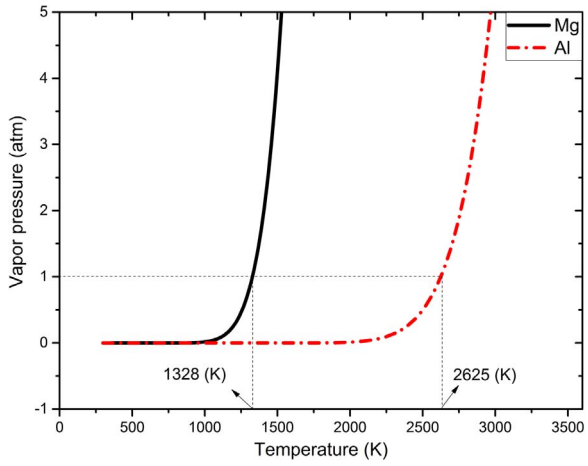

Fig. 2. Vapor pressure variations versus temperature for magnesium and aluminum.

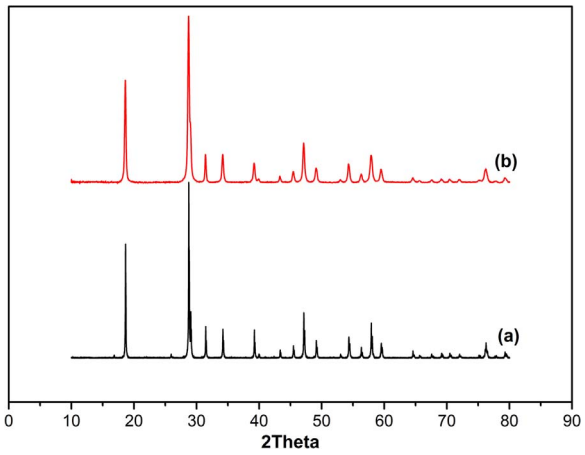

Fig. 3. X-ray diffraction of (a) natural scheelite that is kept in the University of Arizona Mineral Museum (b) synthesized scheelite.

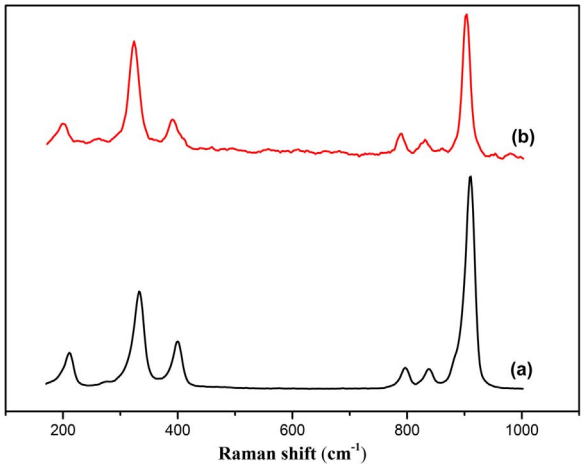

Fig. 4. Raman spectra of (a) natural scheelite that is kept in University of Arizona Mineral Museum (b) synthesized scheelite.

Accordingly, the vapor pressures of magnesium and aluminum versus temperature are presented in Fig. 2. As it can be seen, magnesium vapor pressure is highly sensitive to the temperature. One atmosphere vapor pressure is attained at 1328 K and 2625 K for magnesium and aluminum respectively. In other words, these temperatures represent boiling points of magnesium and aluminum. As mentioned above, the highest adiabatic temperatures are related to the stoichiometric mixtures. Vapor pressure of magnesium at 3533 K is 1600 atm, whereas vapor pressure of aluminum is just 9 atm at 3124 K. This difference affects the mechanism of the process that will be discussed in the next part. It should be noted that thermodynamic calculations cannot predict non-equilibrium processes such as high energy milling or MSR but they can give a general picture of the reactions.

3.2. Characterization of synthesized scheelite

Fig. 3 shows the X-ray diffraction patterns of synthesized and natural scheelite. X-ray diffraction of natural scheelite relates to the sample that is kept in the University of Arizona Mineral Museum [21]. It can be seen that the synthesized scheelite pattern is the same as natural one. In addition, no excess or unidentified peak can be seen in the pattern that represents a pure synthesized scheelite. Fig. 4 shows the raman spectra of these samples. The patterns show a good similarity between two samples. It is reported that the W-O interatomic distance is smaller than Ca-O one and thus the four oxygen atoms surrounding a W atom form a tetrahedron [22]. This suggests three types of vibrations in the scheelite structure. First group consists of internal vibrations of WO_4 ion in which the Ca ions remain stationary. The second group is the vibrations in which the Ca and WO_4 ions (as rigid units) vibrate together and the third group is Ca and oxygen vibrations. The peaks at 931, 838 and 325 relate to the $[WO_4]^{2-}$ vibrations as a rigid unit while the peaks at 795 and 400 represents W-O vibrations. The last peak at 210 shows the Ca-O vibrations [22].

3.3. Temperature monitoring curves

Fig. 5 represents the time dependent temperature variations of the outer wall of milling vial obtained by temperature monitoring system for magnesium containing samples. This figure includes time-temperature curves of the first group of samples milled for 60 min and the second group that is milled until immediately after observing the abrupt temperature increase. Arrows in the figure indicate milling interruption time for each sample. It can be seen that the temperature of the vial increases gradually by running the ball mill. There could be two mechanisms for temperature rise in this step. One is the local temperature pulses due to ball-to-ball, ball-to-powder and ball to wall collisions. These local temperature pulses have a short duration of about 10^{-5} s [23–25] and increase the overall temperature of the system including balls and the vial. In addition, it has been reported that more than 90% of mechanical energy imparted to the powders is transformed into heat and this increases the temperature of powder [26]. It is not possible to measure these local temperature rises

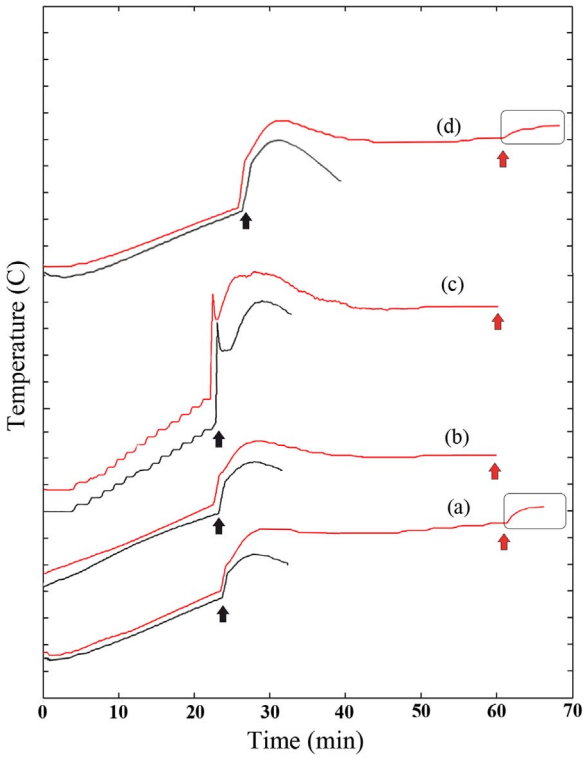

Fig. 5. Time dependent temperature variations of the milling vial for various samples. The tick marks on the temperature scale are 1 °C from each other. (a) 0.8 Mg (b) 1 Mg (c) 1.2 Mg (d) 1.4 Mg.

practically. But it was estimated about several hundred degrees Celsius by calculations considering the amount of plastic deformation and heat transfer conditions [27–29]. Friction is the other reason for temperature increase during milling. Several researchers have investigated the milling of systems containing graphite or molybdenite. It has been reported that the mixtures containing graphite or molybdenite need prolonged activation. It is due to layered crystal structure and lubricating property of these materials that decrease friction during the milling process [30].

There is an abrupt temperature rise in all samples in the range of 20–30 min (Fig. 5). The rate of temperature rise in this step was very high and was measured to be about 50 °C/min, whereas the rate of temperature rise in the early steps of milling was about 0.15 °C/min. So it can be concluded that this abrupt temperature rise is due to a new phenomenon other than the above mentioned mechanisms. This phenomenon is a highly exothermic reaction in the MSR mode that is ignited by mechanical milling. In addition to the powder temperature rise, milling causes crystal imperfections that increase the reactivity and the internal energy of system and subsequently improves needed conditions to provide reaction activation energy.

Secondary peaks can be seen immediately after the MSR ones in 0.8Mg, 1Mg and 1.4Mg samples. The rate of temperature rise in these peaks is significantly lower than MSR peaks. After reaching a maximum value in the secondary peaks, the temperature decreases and finally approaches to a steady-state value determined by the balance between the sources of heat generation in the vial and the heat loss to the environment. The 1.2Mg sample shows a different thermal behavior that can be seen in Fig. 5. There is a temperature drop between MSR peak and secondary peak in this sample.

As mentioned before, similar experiments were carried out on scheelite-aluminum mixtures. Table 1 shows the composition of scheelite-aluminum samples. The time-temperature curves of these samples include 3 main steps similar to scheelite-magnesium ones (the graphs not reported here). First step is gradual temperature rise due to balls collisions and friction. Second step is the abrupt temperature rise due to MSR ignition and the third one is secondary peak that has lower rate of temperature rise.

Different parameters of the time dependent temperature variation diagrams have been compared to realize the mechanism of these behaviors. These parameters are represented in Fig. 6a. These parameters are considered as follow: Ignition time (A), the maximum temperature rise of MSR peak (B), temperature drop immediately after MSR peak (C), temperature rise of secondary peak (D). Additionally, the rate of the temperature increase of the secondary peaks are calculated for all samples.

It can be seen in Fig. 6b that ignition time (A parameter) decreases by increasing Mg or Al content from 0.8 to 1.2 stoichiometry. Increasing the contents of reacting metals to 1.4 stoichiometry have negative effect on parameter A and prolong the ignition time.

Extra scheelite acts as diluent and heat sink in samples containing 0.8 stoichiometry of Mg or Al. Thus by increasing the Mg or Al content, the diluent role of scheelite is eliminated and MSR ignites in shorter time. The same behavior is observed for the samples of 1.4Mg and 1.4Al due to diluent role of reacting metals. In addition, it has been reported that continuous fracturing-welding and or amorphization- recrystallization occur in soft metals with low melting point such as magnesium [25]. These events prevent efficient activation in the samples containing higher amount of metals (1.4Mg and 1.4Al) and consequently ignition time increases.

The ignition in aluminum containing samples need 10–20 min more activation time in comparison to magnesium ones. Various researchers have investigated the parameters affecting ignition time during milling. But they were unable to propose a comprehensive mechanism. This is due to various physical, chemical and thermodynamical properties of elements affecting the ignition time. The magnesium and aluminum powders had similar particle size distribution in the above mentioned experiments. To investigate the effective parameters, similar experiments were carried out by using aluminum powder with particle size distribution smaller than 10 μm. The results showed that ignition occurs in the range of 20–25 min by using finer aluminum powder. Considering the same experimental conditions in both systems of Al and Mg, the different ignition time can be related to thermodynamical characteristics such as lower adiabatic temperature of scheelite-aluminum system. It is also confirmed by Takacs for several systems [10].

Fig. 6c shows parameter B (ΔT of ignition) for samples containing various amounts of Mg or Al. This temperature rise represents the intensity of exothermic reaction. It is seen that by increasing the reacting metal (Mg or Al), a greater amount of heat releases during MSR. Maximum ΔT is reached at the 1.2Mg sample. In the 0.8Mg sample, reaction cannot proceed completely due to off-stoichiometric ratio of reactants. In addition, a fraction of MSR heat is consumed to increase the temperature of extra scheelite. Calculations that are shown in Fig. 1 verify that this sample has lower adiabatic temperature. In the 1Mg sample the reaction proceeds more easily due to higher content of magnesium and consequently more heat releases during MSR. It was mentioned earlier that the scheelite-magnesium mixture with stoichiometric composition (sample 1Mg) has the maximum calculated adiabatic temperature, but opposite results can be seen in Fig. 6c. Adiabatic temperature calculations are in closer agreement with reactions occurring in SHS mode, but it should be noted that MSR is different from SHS process. In SHS systems, the reacting particles are in physical contact completely and the reaction propagates trough a wave along the entire compact. While in MSR mode, powder particles are randomly distributed all over the vial space. Deidda et al. [31] photographed the MSR moment in a transparent vial. He showed that MSR occurs similar to an explosion that may leave unreacted particles in the vial. Additionally it has been reported that powders may be trapped in dead zones that separate them from overall process [10,32]. Therefore the kinetic conditions are not suitable to attain the maximum temperature rise in 1Mg sample.

The ΔT of MSR peak (parameter B) for 1.2Mg sample is 2.5 times

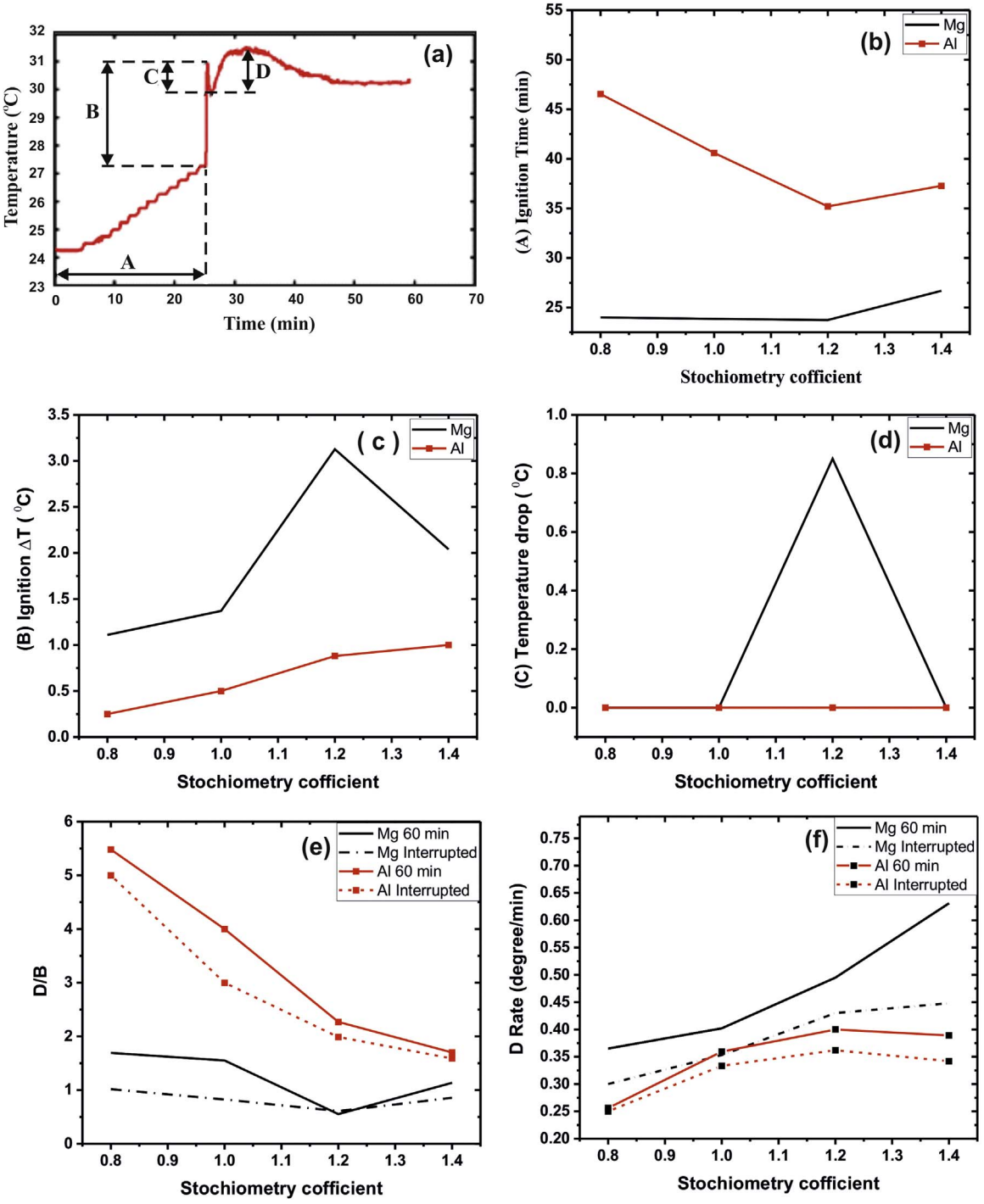

Fig. 6. Parameters extracted form time dependent temperature variations diagrams (a) indication of different parameters in time dependent temperature diagram (b) ignition time (c) the amount of temperature rise in MSR peak (d) the amount of temperature drop immediately after ignition peak (e) ΔT of secondary peak / ΔT of MSR peak (d) the temperature increase rate in secondary peak.

higher than previous samples (Fig. 6c). Thus it can be concluded that MSR proceeds farther in the 1.2Mg sample in comparison to samples containing lower amounts of magnesium. Fig. 7 shows X-ray diffraction patterns for samples obtained immediately after MSR and after 60 min of milling.

As it can be seen in XRD patterns of samples milled until ignition observation, the 100% peak of scheelite (at $2\theta = 29^{\circ}$) is shortened by increasing Mg content in the mixtures. This means more proceeding of reaction and consequently release of higher amount of heat during MSR. Thus ΔT of MSR (parameter B) increases by increasing Mg content. ΔT of ignition for the 1.4Mg sample is more than that of the 0.8Mg and 1Mg samples but lower than the 1.2Mg. The highest ΔT of MSR (parameter B) is 3 °C and relates to the 1.2Mg sample.

Similar to scheelite-magnesium mixtures, the parameter B is also increased by increasing aluminum content in scheelite-aluminum samples. The amount of parameter B is between 0.25 and 1 °C for scheelite-aluminum group while it is in the range of 1–3 °C for scheelite-magnesium group. The higher reaction heat of scheelite-magnesium system could be one of the reasons for higher amounts of parameter B in comparison to the scheelite-aluminum mixtures.

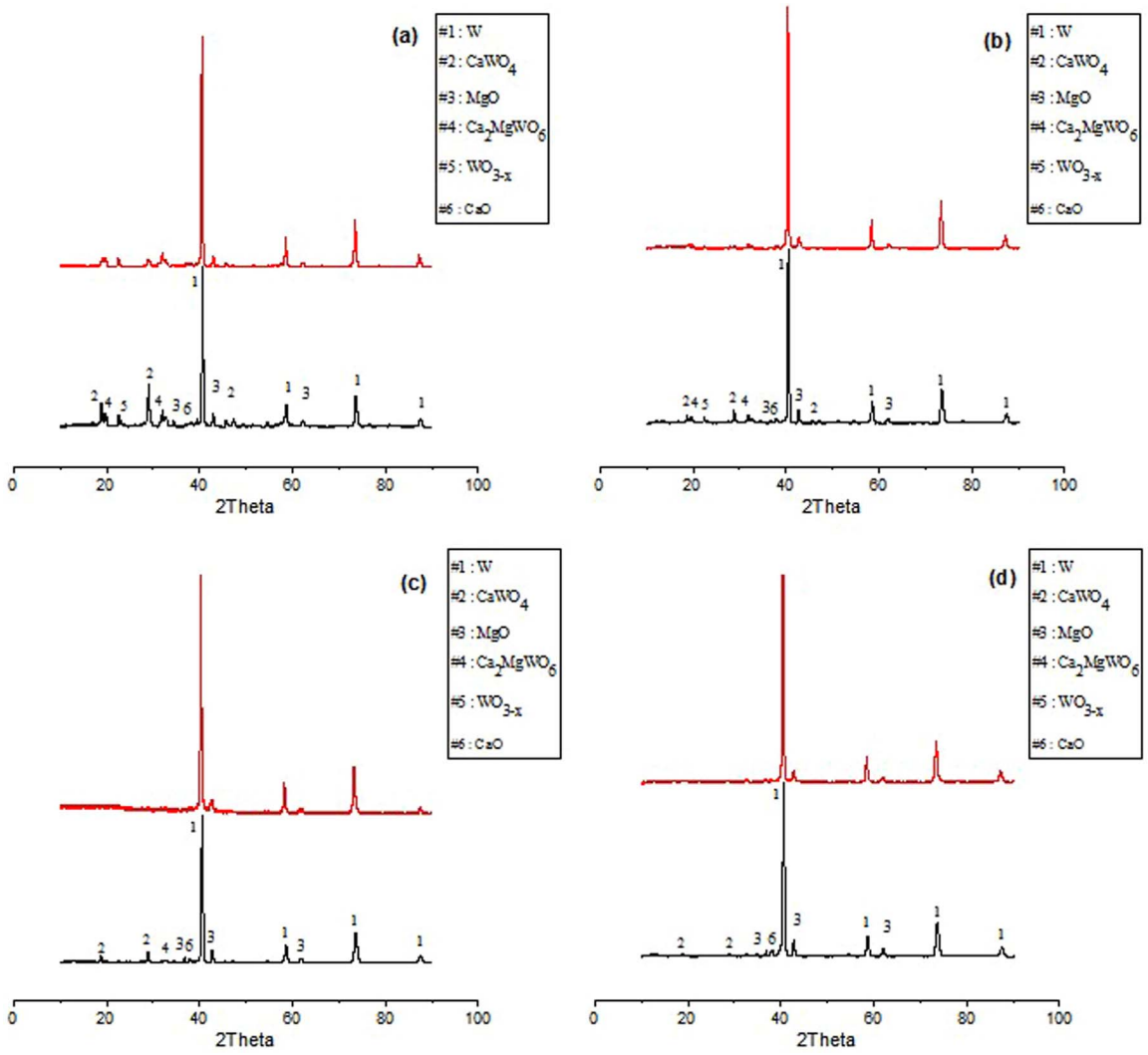

Fig. 7. X-ray diffraction patterns of samples milled until ignition observation (black) and milled for 60 min (red) (a) 0.8Mg (b)1Mg (c) 1.2Mg (d) 1.4Mg. (For interpretation of the references to color in this figure legend, the reader is referred to the web version of this article.)

Fig. 6e shows the ratio of secondary temperature rise to MSR temperature rise (D/B). D/B decreases with increasing reacting metals in both groups. The 1.2Mg and 1.2Mg60 samples have the lowest D/B ratio. It can be seen that the D/B ratio of the Al group has higher values. It means that MSR is weaker in Al containing samples and residual materials react gradually during subsequent milling. This could the other reason for higher amounts of parameter B in scheelite-magnesium mixtures.

Fig. 6f shows the rate of temperature rise of the secondary peak for samples milled for 60 min and until ignition observation. It can be seen that the rate of temperature increase in secondary peak increases with increasing magnesium content. The rate of temperature rise in secondary peak for all samples milled for 60 min is higher than samples milled until the observation of ignition. In scheelite-aluminum mixtures, the rate of temperature rise increases with increasing Al content from 0.8 to 1.2 stoichiometry, but addition of more than 1.2 stoichiometry aluminum has negative effect on the rate in secondary peak.

We have to know the mechanism of heat generation during milling process to interpret these events. The first heat source, as mentioned before, is friction and collision of balls with walls, powders and other balls. Thus it is obvious that this heat generation source is interrupted, when the ball mill is turned off. Hence D/B ratio and the rate of temperature rise in secondary peak is lower for samples milled until ignition observation. Second heat generation source is highly exothermic reaction that occurs during milling process. As mentioned earlier, abrupt temperature increase was the indication for this exothermic reaction.

The other source of heat generation in secondary temperature rise is gradual reaction of residual reactants. Fig. 7 shows the X-ray diffraction of samples milled for 60 min and until ignition observation. Unreacted scheelite can be seen in samples obtained by interruption of milling process immediately after MSR. With continued milling until 60 min the scheelite peaks are shortened or disappeared completely. So the heat of gradual reaction between scheelite and magnesium is the other source of heat for secondary temperature rise of samples milled until 60 min.

As mentioned before the temperature of balls increases during milling due to collisions and friction. Thus the temperature of balls increases with milling time due to increase in the number of collisions. Because of point contacts between balls and vial during milling, the difference in the temperature between inside and outside of vial could be significant. Kwon et al. [24] has measured the temperature of balls immediately after interruption of milling by using a calorimeter. He has reported the temperature of balls in the range of 100–600 °C depending on milling conditions. It should be noted that there was not any exothermic reaction in their systems and these temperatures were attained just through collision and friction. The permanent motion of the balls decrease heat exchange of balls through conduction. Thus interrupting

the mill let the balls to conduct their heat to the ambient. The temperature rises pointed by rectangles in Fig. 5 shows this effect. It can be seen that the temperature increased immediately after stopping the mill. Thus it can be concluded a part of the secondary temperature rise relates to this effect in samples milled until immediately after ignition.

The temperature drop between MSR and the secondary peak is the unexplained part in the time-temperature curve of 1.2Mg sample. Few researchers have reported similar thermal patterns, but there isn't any rational explanation for the reasons of these behaviors in published papers. Al-I, Zr-2S and Ni-P are systems that have shown similar temperature patterns during reactive milling [10,11,33]. The reported temperature behavior of Ni-P system was quite similar to the 1.2Mg time-temperature curve in the present study. The main similarity between these systems is the presence of a high vapor pressure reactant. Vapor pressure of iodine, sulfur and phosphor is equal to 1 atm at 184, 445 and 280 °C respectively. As previously mentioned, this vapor pressure is reached at 1090 °C for magnesium. Based on these explanations, a hypothesis suggested that the sublimation and deposition of high vapor pressure reactant is the reason for the observed temperature behavior. As previously stated, aluminum has very low vapor pressure in comparison to the magnesium. Hence making a comparison between scheelite-aluminum and scheelite-magnesium temperature behaviors can be useful to confirm the hypothesis. In addition, it was tried to obtain evidences about sublimation-deposition of magnesium in 1.2Mg sample. To attain this target, the O-rings of the milling vial were modified to generate a safe zone on the cap to gather probable depositions. The frequency of collisions is lower in this area, hence probable magnesium vapor can deposit as a uniform layer on the inner surface of the cap. This safe zone can act as a nucleation area for deposition of probable magnesium vapor due to temperature difference between gas and vial wall.

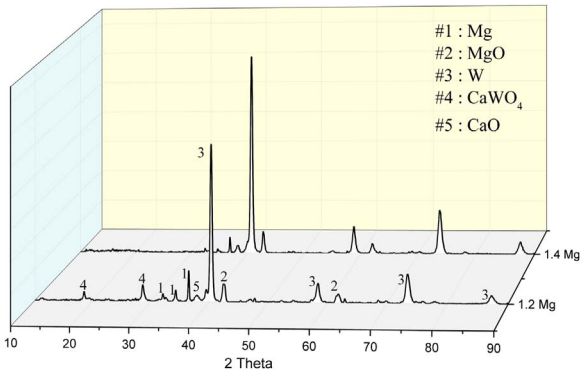

Fig. 9. X-ray diffraction pattern of deposited powder on the cap for 1.2Mg and 1.4Mg samples.

Fig. 8a shows different zones on the clear cap of vial. Fig. 8b and c represent the cap for 0.8Mg and 1Mg samples. It is seen that the safe zone is free from any deposition. The zone of ball impacts can be seen as a dark ring in outer part of cap. The area indicated by red line in Fig. 8d represents formation of deposit for 1.2Mg sample. It should be noted that the color of the deposit whitened rapidly immediately after opening the vial. X-ray diffraction pattern of deposit is shown in Fig. 9. Metallic magnesium and magnesium oxide are the dominate phases in

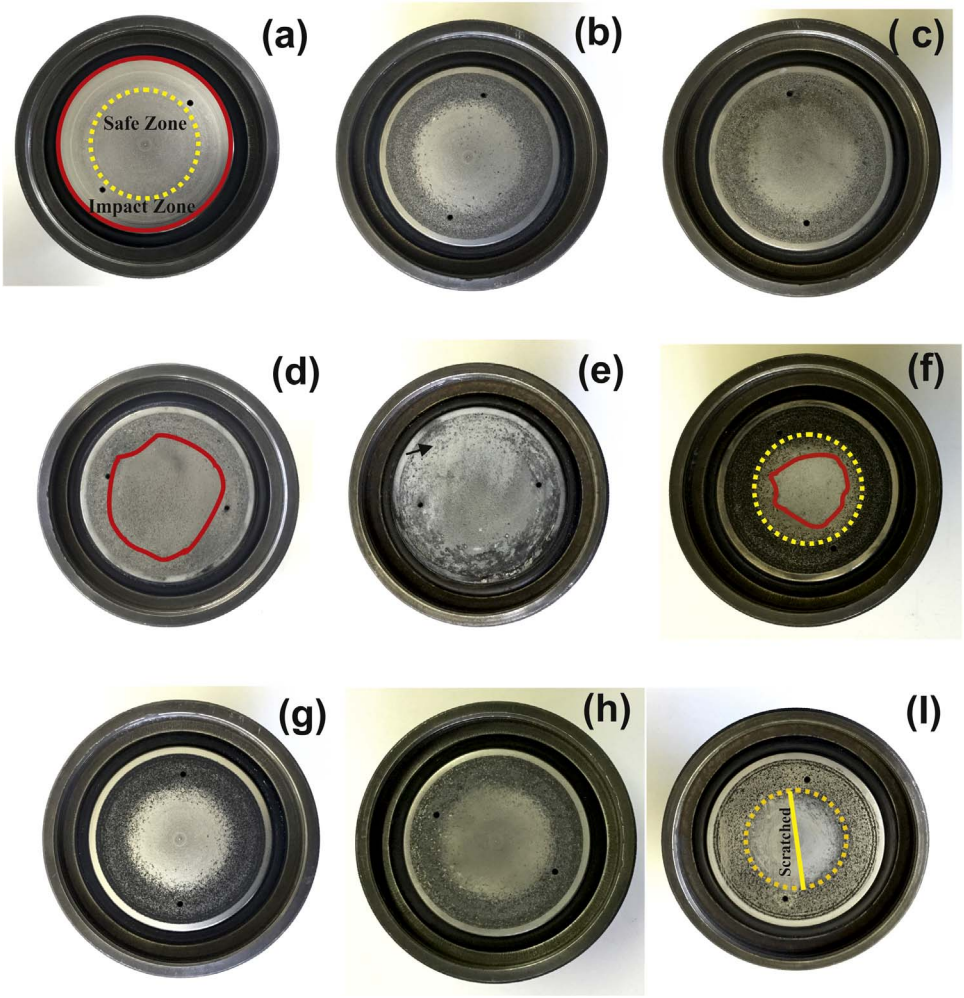

Fig. 8. Inner surface of Cap for different samples, (a) clean surface, safe zone and impact zone are indicated, (b) the cap for 0.8Mg sample, (c) the cap for 1Mg sample, (d) the cap for 1.2Mg sample, red line indicates deposition, (e) the cap for 1.4Mg sample, arrow indicates deposition formation even in impact zone, (f) the cap for 1.4Mg60 sample, red line shows remained deposition after 60 min of milling, (g) the cap for 0.8Al sample, (h) the cap for 1.2Al sample, (i) the cap for 1.4Al sample. (For interpretation of the references to color in this figure legend, the reader is referred to the web version of this article.)

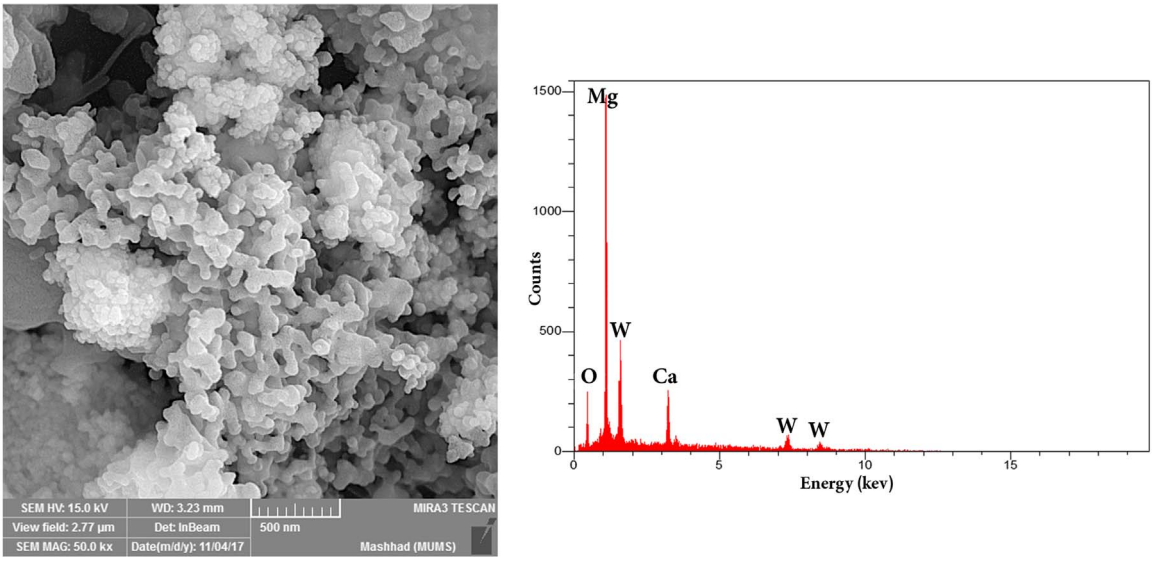

Fig. 10. FESEM micrograph and EDX analysis of deposited powder on the cap after MSR for 1.2Mg sample.

the deposited powder. The deposit contains 34.7 Mg, 27.7MgO, 24.8 W, 6.9% CaWO4 and 5.9% CaO according to the quantitative analysis of XRD pattern. As it was shown in Fig. 7c, there is not any metallic magnesium in milled 1.2Mg sample (Fig. 7c), while there is a significant amount of metallic magnesium and magnesium oxide in deposited powder. Particles are suspended in the vial during milling, so they entrap in the deposited gas when the magnesium transforms to solid. That's why we see tungsten phase in deposition. Fig. 10 shows FESEM micrograph and EDX spectra of deposit. A porous and interwoven structure can be seen, while MSR products are very fine and shapeless. EDX spectra show the dominating presence of magnesium in the structure of the deposit. Fig. 8e shows the cap for 1.4Mg samples. Deposited powder can be seen all over the cap even in impact zone that indicates the sublimation of magnesium during MSR. The amount of deposited powder in this sample is five times more than the deposition of 1.2Mg sample. XRD of deposited powder for 1.4Mg sample also shows the presence of metallic magnesium (Fig. 9). Red line in Fig. 8f indicates remained deposit after 60 min milling that shows that the deposited magnesium blends back into the milling process and participates in subsequent gradual reaction with scheelite.

Fig. 8g, h and i show the cap for 0.8Al, 1.2Al and 1.4Al samples. There is not any deposition on the cap immediately after MSR. A very thin layer can be seen in 1.4Al sample that was whitened immediately after exposing to the atmosphere. The amount of this layer was too low for sampling. This layer could be aluminum that forms due to partial evaporation of Al due to high excess amount in 1.4Al sample.

According to these facts we can explain the mechanism of temperature variations. In 0.8Mg60 and 1Mg60 samples, MSR does not progress completely. The primary reason of secondary temperature rise in these samples is gradual exothermic reaction of remained reactants. The larger amounts of D/B ratio are related to the significant role of gradual reaction in heat generation in comparison to MSR. Sublimation-deposition of magnesium was not seen in these samples due to lower amount of reacting metal.

MSR occurs with highest intensity in the 1.2Mg60 sample and releases a large amount of heat that increases the temperature of vial to the maximum value. A portion of the heat, sublimes excess magnesium and therefore all reactions stop in the system. Due to high temperature rise in MSR step, other heat sources are incapable of supplying needed heat to continue the increasing trend of the temperature rapidly and consequently the temperature begins to drop. The deposited magnesium is blended back to the process and gradual reaction starts with delay. It needs to mix and activate again and hence gradual reaction begins with delay. The delay time in the present study was about 100 s. The lowest D/B ratio is attained in this sample due to high temperature rise of MSR peak.

As mentioned before MSR proceeds more in previous samples in 1.4Mg60. The released heat sublimes high excess amount of magnesium and thus the temperature would not increase. Due to the lower temperature rise, other sources can provide the needed heat; therefore, there is not any temperature drop after MSR peak in this sample. Additionally, deposition of magnesium is exothermic and this could be the other source of heat generation in this sample. That's why the 1.4Mg sample has highest rate of temperature rise in the secondary peak.

D/B ratio is so larger in aluminum containing samples that illustrates weak MSR and outstanding role of post-MSR gradual exothermic reaction. This ratio decreases and getting close to the magnesium D/B amounts by increasing aluminum content. This means higher conversion of scheelite during MSR. Sublimation-deposition in aluminum containing samples was not seen due to low vapor pressure of aluminum. The main reason for secondary temperature increase of all samples milled until MSR is outflow of heat from system. The temperature increase rate in secondary peak and D/B are lower for these samples.

3.4. Chemical mechanism

Fig. 11 shows X-ray diffraction pattern of 1.2Mg sample milled at various time intervals. No new phase formation can be seen in these patterns prior to ignition. The peaks have become broader and shorter. Additionally, the peaks have shifted to lower Bragg angels. This is due to increase in density of crystal imperfections, lattice strain and also crystal refinement. There are investigations about the mechanism of this step. Oghenevweta et al. [34] reported nanoscale nucleation of products prior to ignition formed by solid-state diffusion of reactant atoms. The size of nuclei was reported to less than 10 nm that were measured by HRTEM. The milling process increases the size and number of these nuclei to a critical value that causes the occurrence of ignition. Similar events can occur in the present process prior to ignition. XRD pattern of the powder immediately after MSR can be seen in Fig. 11. The dominate phases are metallic tungsten and magnesium oxide. There is a short peak of scheelite in this sample that has been disappeared in XRD pattern of the sample milled for 60 min (Fig. 11).

Investigating the mechanism of SHS reactions is too hard due to rapid propagation. The main methods that have been reported in papers are combustion front quenching and in situ synchrotron radiation

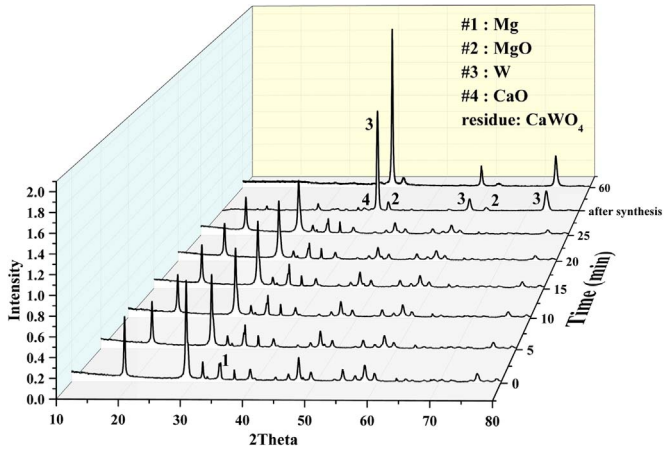

Fig. 11. X-ray diffraction patterns of 1.2Mg sample milled at various time intervals.

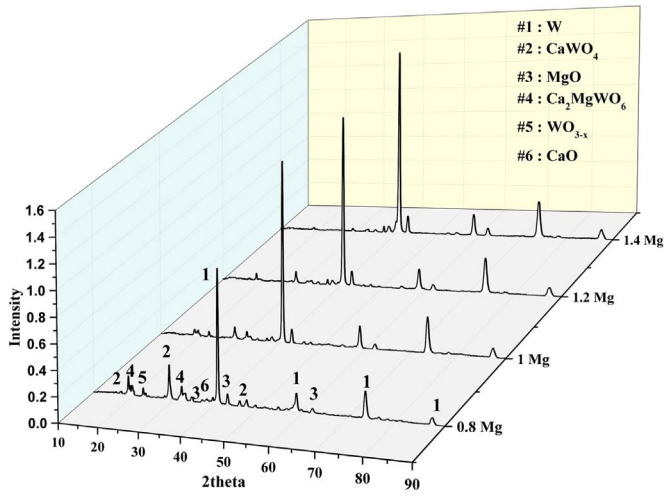

Fig. 12. XRD patterns of samples containing various amount magnesium immediately after MSR.

technique [35,36]. Front quenching method is based on increase in heat losses and consequently rapid extinction of reaction front to identifying probable intermediate species and phase transformations. The use of these methods in MSR process is practically impossible. Therefore we tried to stop the reactions by using off-stoichiometric mixtures. Excess materials in these mixtures act as heat sinks that increase the heat losses.

Fig. 12 shows XRD patterns of samples milled until immediately after MSR. Several peaks can be seen in XRD pattern of 0.8Mg that shorten or disappear by increasing the Mg content or continuing milling process (Fig. 7). A group of these peaks relate to the Ca_2MgWO_6 phase. Additionally, a group of overlapping peaks are seen in the range of $2\theta = 23^{\circ}$. This range relates to the spectra of partially reduced tungsten oxides such as $W_{25}O_{73}$, $W_{24}O_{68}$, $W_{14}O_5$, $W_{18}O_{49}$, $W_{17}O_{47}$ and WO_2. Milling and MSR are non-equilibrium processes and make various crystal imperfections that demonstrate as peak shifts to the lower or higher Bragg angles. In addition, the spectra of partially reduced tungsten oxides are quite similar and the 100% peak of them located in the range of $2\theta = 23^{\circ}$. Due to these problems it is impossible to assign these peaks to a phase definitely. Thus we have indicated these peaks as $WO_{3-}x$ where $0 < x < 1$.

According to the XRD patterns, reaction sequence of scheelite and magnesium mixtures can be explained as below:

$$3\ CaWO_4 + 6\ Mg \rightarrow Ca_3WO_6 + 2\ W + 6\ MgO$$

$$Ca_3WO_6 + x\ Mg \rightarrow WO_{3-x} + 3\ CaO + x\ MgO\ (0 < x < 1)$$

$$WO_{3-x} + (3 - x)\ Mg \rightarrow W + (3 - x)\ MgO$$

In samples with lower content of magnesium tricalcium tungstate reacts with magnesium oxide according to the following reaction:

$$Ca_3WO_6 + MgO \rightarrow Ca_2MgWO_6 + CaO$$

To ensure the sequential progress of reactions in samples with higher content of magnesium, the combustion front of a 1.2Mg pellet was quenched. $WO_{3-}x$ peaks were seen in XRD pattern of quenched front that prove sequential mode in samples with higher content of magnesium.

Fig. 13 shows AFM micrograph of tungsten powder. It is seen the particle size of products is smaller than 50 nm. It is obvious that nano-particle tungsten metal can lead to the synthesis of nano particle tungsten carbide in the presence of carbon.

4. Conclusion

The idea of this study is the production of tungsten carbide using scheelite through mechanically-induced self-propagating reaction. This process includes two steps. The first is synthesis of tungsten via MSR and the second is gradual reaction of tungsten and carbon during subsequent milling. This study has investigated the mechanism of the first step. The milling mechanism of scheelite-magnesium mixtures is described using in-situ temperature monitoring, FESEM and X-ray diffraction analysis. Based on time dependent temperature variations diagrams, the milling process consists of 3 steps. The first is

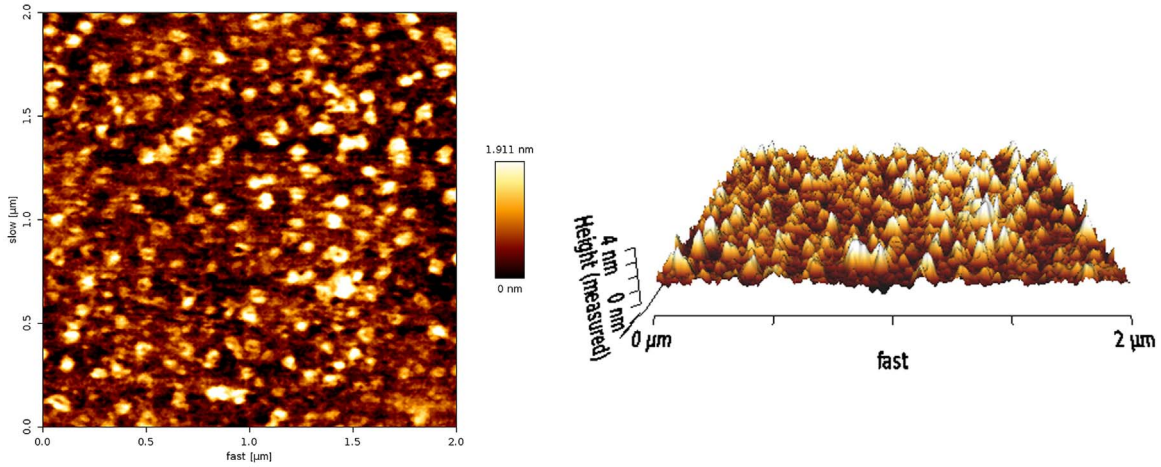

Fig. 13. AFM micrograph of 1.2Mg sample milled for 60 min.

temperature rise due to collision of balls and friction. The second is an abrupt temperature rise due to exothermic reaction of scheelite and magnesium. There was a secondary temperature peak after MSR in all samples due to gradual reaction of remained reactants. A comparison was made between scheelite-magnesium and scheelite-aluminum milling behaviors to interpret the variation of temperature as a function of time. Sublimation-deposition of magnesium was seen in samples containing higher amount of magnesium. The sequence of scheelite-magnesium reaction appears to be $CaWO_4 \rightarrow Ca_3WO_6 \rightarrow Ca_2MgWO_6 \rightarrow WO_{3-}x \rightarrow W$.

Acknowledgments

This research was supported by Ferdowsi University of Mashhad, Iran under the Grant No. 3/42276.

References

[1] E. Lassner, W.-D. Schubert, Tungsten, Properties, Chemistry, Technology of the Element, Alloys, and Chemical Compounds, Kluwe Academic/Plenum Publishers, New york, USA, 1999, p. 422.
[2] S. Norgren, et al., Trends in the P/M hard metal industry, Int. J. Refract. Met. Hard Mater. 48 (Supplement C) (2015) S31–S45.
[3] S.N. Bhosale, S. Mookherjee, R.M. Pardeshi, Current practices in tungsten extraction and recovery, High Temp. Mater. Process. (1990) 9.
[4] E. Lassner, et al., Tungsten, Tungsten Alloys, and Tungsten Compounds, Ullmann's encyclopedia of industrial chemistry, 1996.
[5] T. Brown, P. Pitfield, *Tungsten.* Critical Metals Handbook, (2013), pp. 385–413.
[6] E. Lassner, From tungsten concentrates and scrap to highly pure ammonium paratungstate (APT), Int. J. Refract. Met. Hard Mater. 13 (1–3) (1995) 35–44.
[7] G. Schaffer, P. McCormick, Reduction of metal oxides by mechanical alloying, Appl. Phys. Lett. 55 (1) (1989) 45–46.
[8] G. Schaffer, P. McCormick, Displacement reactions during mechanical alloying, Metall. Trans. A 21 (10) (1990) 2789–2794.
[9] L. Takacs, V. Soika, P. Baláž, The effect of mechanical activation on highly exothermic powder mixtures, Solid State Ion. 141 (2001) 641–647.
[10] L. Takacs, Self-sustaining reactions induced by ball milling, Prog. Mater. Sci. 47 (4) (2002) 355–414.
[11] L. Takacs, Multiple combustion induced by ball milling, Appl. Phys. Lett. 69 (3) (1996) 436–438.
[12] L. Takacs, S. Mandal, Preparation of some metal phosphides by ball milling, Mater. Sci. Eng.: A 304 (2001) 429–433.
[13] M. Sakaki, et al., Control of carbon loss during synthesis of WC powder through ball milling of WO 3–C–2Al mixture, J. Alloy. Compd. 486 (1) (2009) 486–491.
[14] M.S. Bafghi, et al., Evaluation of process behavior and crystallite specifications of mechano-chemically synthesized WC–Al 2 O 3 nano-composites, Mater. Res. Bull. 49 (2014) 160–166.
[15] A. Heidarpour, N. Shahin, S. Kazemi, A novel approach to in situ synthesis of WC-Al_2O3 composite by high energy reactive milling, Int. J. Refract. Met. Hard Mater. 64 (Supplement C) (2017) S1–S6.
[16] M. Sakaki, et al., Conversion of W 2C to WC phase during mechano-chemical synthesis of nano-size WC–Al_2O_3 powder using WO 3–2Al–(1 + x) C mixtures, Int. J. Refract. Met. Hard Mater. 36 (2013) 116–121.
[17] N.J. Welham, Formation of micronised WC from scheelite (CaWO4), Mater. Sci. Eng.: A 248 (1) (1998) 230–237.
[18] N. Novikov, I. Borovinskaya, Combustion in Chemical Engineering and Metallurgy, ed A.G. Merzhanov. Chernogolovka, Moscow, 1975, pp. 174–188.
[19] A.G. Merzhanov, Self-propagating high-temperature synthesis: twenty years of search and findings, Combust. Plasma Synth. High-Temp. Mater. (1990) 1–53.
[20] Z.A. Munir, U. Anselmi-Tamburini, Self-propagating exothermic reactions: the synthesis of high-temperature materials by combustion, Mater. Sci. Rep. 3 (7–8) (1989) 277–365.
[21] B. Lafuente, et al., The Power of Databases: the RRUFF Project, in Highlights in Mineralogical Crystallography. Walter de Gruyter GmbH, 2016.
[22] J. Russell, R. Loudon, The first-order Raman spectrum of calcium tungstate, Proc. Phys. Soc. 85 (5) (1965) 1029.
[23] D.R. Maurice, T. Courtney, The physics of mechanical alloying: a first report, Metall. Trans. A 21 (1) (1990) 289–303.
[24] Y.-S. Kwon, K.B. Gerasimov, S.-K. Yoon, Ball temperatures during mechanical alloying in planetary mills, J. Alloy. Compd. 346 (1) (2002) 276–281.
[25] C. Suryanarayana, Mechanical Alloying and Milling, CRC Press, 2004.
[26] L.Y. Pustov, Kaloshkin. S.D., V.V. Tcherdyntsev, I.A. Tomilin, E.V. Shelekhov, A.I. Salimon, Experimental Measurement and Theoretical Computation of Milling Intensity and Temperature for the Purpose of Mechanical Alloying Kinetics Description. in Mater. Sci. Forum, 2001.
[27] R.B. Schwarz, C.C. Koch, Formation of amorphous alloys by the mechanical alloying of crystalline powders of pure metals and powders of intermetallics, Appl. Phys. Lett. 49 (3) (1986) 146–148.
[28] R.M. Davis, C. Koch, Mechanical alloying of brittle components: silicon and germanium, Scr. Metall. 21 (3) (1987) 305–310.
[29] T. Courtney, Process modeling of mechanical alloying (overview), Mater. Trans. JIM 36 (2) (1995) 110–122.
[30] H. Shalchian, et al., On the mechanism of molybdenite exfoliation during mechanical milling, Ceram. Int. 43 (15) (2017) 12957–12967.
[31] C. Deidda, F. Delogu, G. Cocco, In situ characterisation of mechanically-induced self-propagating reactions, J. Mater. Sci. 39 (16–17) (2004) 5315–5318.
[32] Z.-G. Yang, L. Shaw, Synthesis of nanocrystalline SiC at ambient temperature through high energy reaction milling, Nanostruct. Mater. 7 (8) (1996) 873–886.
[33] L. Takacs, Self-sustaining reactions induced by ball milling: an overview, Int. J. self-Propagating High-Temp. Synth. 18 (4) (2009) 276–282.
[34] J. Oghenevweta, D. Wexler, A. Calka, Early stages of phase formation before the ignition peak during mechanically induced self-propagating reactions (MSRs) of titanium and graphite, Scr. Mater. 122 (2016) 93–97.
[35] C. Gras, et al., In situ synchrotron characterization of mechanically activated self-propagating high-temperature synthesis applied in Mo–Si system, Acta Mater. 47 (7) (1999) 2113–2123.
[36] A.G. Merzhanov, The chemistry of self-propagating high-temperature synthesis, J. Mater. Chem. 14 (12) (2004) 1779–1786.